

# Tensile forces induced in collagen by means of electromechanochemical transductive coupling\*

A. J. Grodzinsky<sup>†</sup> and N. A. Shoenfeld

Continuum Electromechanics Laboratory, Department of Electrical Engineering and Computer Science, Massachusetts Institute of Technology, Cambridge, Massachusetts 02139, USA  
(Received 20 October 1976)

Electric fields are applied across a charged collagen membrane which supports a gradient in neutral salt concentration. Experiments over a wide range of concentration have shown that isometric tensile force densities larger than that of striated muscle can be induced by the applied field. The experimental results, together with the trends predicted by a theoretical model, suggest that the forces result from field-induced changes in intramembrane salt concentration which in turn modify the internal double layer repulsive forces between charged fibrils. Characteristic times for this electromechanochemical transduction process are examined in terms of the various rate limiting processes of importance.

## INTRODUCTION

Experiments with collagen membranes have been performed which demonstrate the feasibility of a transduction process whereby mechanical work is performed at the expense of chemical energy under the control of an applied electric field. While the ultimate goal is the design and fabrication of implantable devices, the experiments have immediate relevance concerning transduction processes in, and physicochemical characterization of, native and synthetic biopolymers at the macromolecular level. Several mechanochemical energy conversion systems have been studied previously, including those concerning chemical and thermal melting of collagen fibres<sup>1-3</sup> and charge-mediated dimensional changes in random-coil poly(carboxylic acid) gels and ribbons<sup>4</sup>. Our previous experiments<sup>5</sup> with oriented, lightly crosslinked collagen fibres in aqueous media have focused on changes in isometric force mediated by the lateral repulsion of electrical double layers associated with the charged fibrils.

A new electromechanochemical transduction process, involving electric fields applied across collagen membranes which support concentration gradients, is now under investigation. Experiments performed in an isometric configuration over a wide range of pH and ionic strength have shown that the applied field  $\vec{E}_0$  produces changes in tensile force. It is believed that  $\vec{E}_0$  induces changes in the intramembrane electrolyte concentration which then produce the measured changes in force, in a manner similar to that previously observed with collagen fibres<sup>5</sup>. The experimental results agree with the trends of a theoretical derivation based on such a hypothesis. The function of the field  $\vec{E}_0$  is essentially that of a switch to make possible fast, localized con-

trol of electrolyte concentration and induced tensile forces.  $\vec{E}_0$  can lead to several other mechanisms which might induce tensile forces, such as a purely electromechanical coupling of an electrokinetic nature, or an induced change in bath pH due to electrode processes. Experiments have therefore been devised to distinguish between these phenomena and that believed to be at work here. A comparison of the various rate processes and induced force magnitudes associated with these differing processes is given, suggesting the advantages and disadvantages of each as a potential transduction mechanism. Finally, it has also been found that the degree of fibril orientation in the specimen is an important parameter in the determination of the total available force density.

## THEORY

It has been found<sup>5</sup> that isometric force densities larger than that of striated muscle<sup>6</sup> can be induced in oriented collagen fibres in a homogeneous electrolyte bath either by varying pH and hence collagen charge, or by varying neutral salt concentration at constant, non-isoelectric pH. Both procedures vary the magnitude of lateral repulsion forces, i.e. forces perpendicular to the fibre axis, between the double layers of the axially oriented, charged fibrils. These lateral forces are converted by the crosslinked fibril matrix to changes in axial force density as large as 30–40 kgf/cm<sup>2</sup> (see Figures 3–4)<sup>5</sup>. In order to investigate electric field-control of such mechanochemical processes, the experimental transducer configuration shown schematically in Figure 1 was used in the present work. A tubular collagen membrane of thickness  $\delta$  separates inner and outer baths,  $c_0^2$  and  $c_0^1$  respectively, of equal, non-isoelectric pH but of two different neutral salt concentrations, e.g.  $c_0^2 > c_0^1$ . Thus the membrane contains fixed, dissociated charge species as well as mobile ions. An electric field  $\vec{E}_0$  can be applied perpendicular to the tube axis by means of concentric cylindrical platinum electrodes, one inside the collagen tube and the other surrounding it. Inner and outer electro-

\* Presented at the First Cleveland Symposium on Macromolecules, Structure and Properties of Biopolymers, Case Western Reserve University, Cleveland, Ohio, USA, October 1976.

<sup>†</sup> Visiting Lecturer, Department of Orthopedic Surgery, Harvard Medical School and Children's Hospital Medical Center, Boston, Massachusetts 02115, USA. Correspondence should be addressed to Professor Grodzinsky at MIT.

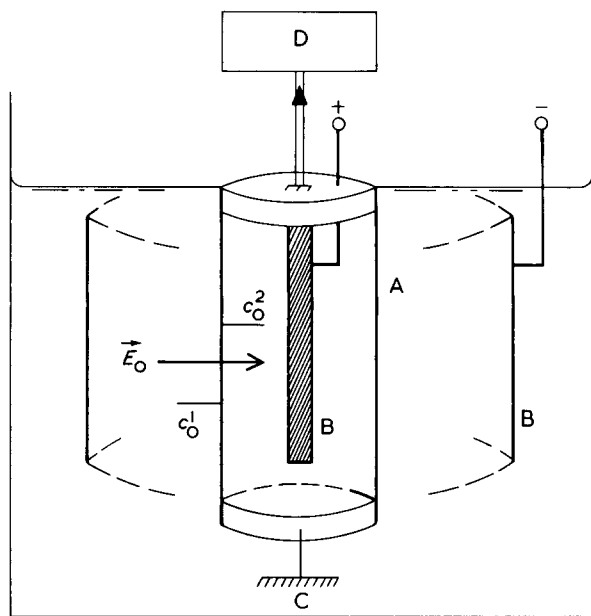


**Figure 1** Schematic representation of specimen mounting and electrode configuration for isometric electromechanochemical transducer experiments. Electric field  $\vec{E}_0$  directed perpendicular to cylindrical membrane axis. Inner and outer electrolyte baths are continually recirculated from large reservoirs (not shown). With  $\vec{E}_0 = 0$  and  $c_0^1 = c_0^2$  the same configuration is used to measure isometric force versus pH or neutral salt concentration. A, Tubular collagen membrane; B, inner and outer platinum cylindrical electrodes; C, fixed support; D, strain gauge

lyte are continually renewed (not shown in *Figure 1*).

With  $\vec{E}_0 = 0$ , the steady state mobile ion concentration profile is defined by the physical constraints of the system and by the limiting boundary concentrations  $c_0^1$  and  $c_0^2$ . Because the concentration varies smoothly from the inner to the outer edge of the membrane, the lateral electrical repulsion forces vary in a similar fashion. Therefore the axial force per unit radial thickness will also vary smoothly. The total equilibrium ( $\vec{E}_0 = 0$ ) axial force is then the sum of the forces per unit thickness from inner to outer edge. If the application of  $\vec{E}_0 \neq 0$  leads to an altered concentration profile, the force profile and hence total force will change concomitantly. Such device operation applies for the case of an induced change in neutral salt concentration only, with membrane charge unaltered in the process.

The mobile ion concentration profiles inside the membrane are determined by a balance between the competing processes of ion migration due to  $\vec{E}_0$ , ion diffusion due to the imposed concentration gradient, and convection of mobile species in the advent of fluid flow through the membrane. Solution of such a problem has been widely investigated with respect to fixed-charge membrane models and the theory of transmembrane potentials.<sup>7-10</sup> The additional possibility that an applied electric field can cause an electrokinetic movement of the membrane if it is non-rigid and deformable must also be included<sup>11</sup>, as well as the possibility of a field-induced convective flow of fluid in and across the membrane (e.g. electro-osmosis)<sup>11,12</sup>. The role of such fluid flow in the determination of intramembrane concentration profile has been investigated<sup>12</sup> with respect to a class of rigid membrane phenomena involving the oscillatory behaviour of pressure and potential drops and fluid and mobile carrier flow; tensile forces were not of interest.

In order to delineate the way in which  $\vec{E}_0$  can alter the

concentration profile in a moving, deformable membrane, we formulate the problem for the simple case of a uniformly charged membrane supporting a gradient in the concentration of a single mono-valent electrolyte such as NaCl. The outer and inner concentrations are the bulk concentrations defined as  $c_0^1 \equiv c_{+0}^1 = c_{-0}^1$  and  $c_0^2 \equiv c_{+0}^2 = c_{-0}^2$  respectively, as shown in *Figure 1*. Though not necessary in this case<sup>17</sup>, it is assumed for simplicity that the diffusion coefficients inside the membrane,  $\bar{D}_+$  and  $\bar{D}_-$ , as well as the ionic mobilities  $\bar{u}_+$  and  $\bar{u}_-$ , are constant. For an incremental volume in the frame of the movable membrane, the continuity relations for mobile positive and negative species in the membrane,  $\bar{c}_+$  and  $\bar{c}_-$ , are ( $z_+ = |z_-| = 1$ ):

$$\frac{D\bar{c}_+}{Dt} = -\frac{1}{F} \nabla \cdot \vec{J}'_+ \quad (1)$$

$$\frac{D\bar{c}_-}{Dt} = +\frac{1}{F} \nabla \cdot \vec{J}'_- \quad (2)$$

where  $F$  is the Faraday constant,  $J'_+$  and  $J'_-$  are the respective ion current densities in the membrane frame, and the convective derivative

$$\frac{D}{Dt} = \frac{\partial}{\partial t} + \vec{v}_m \cdot \nabla$$

$\vec{v}_m$  being the membrane velocity; the right-hand terms in equations (1) and (2) involve carrier fluxes in the membrane frame. In general, additional terms can be added to equations (1) and (2) to account for chemical reactions in the membrane which would lead to production or depletion of the mobile species. Here, we assume for simplicity that the monovalent electrolyte of interest does not react with or bind to any groups in the collagen.

The current densities are written, accounting for diffusion, migration and fluid convection with respect to the movable membrane:

$$\vec{J}'_+ = -F\bar{D}_+ \nabla \bar{c}_+ + F\bar{u}_+ \bar{c}_+ \vec{E}(\vec{r}) + F\bar{c}_+ (\vec{v} - \vec{v}_m) \quad (3)$$

$$\vec{J}'_- = +F\bar{D}_- \nabla \bar{c}_- + F\bar{u}_- \bar{c}_- \vec{E}(\vec{r}) - F\bar{c}_- (\vec{v} - \vec{v}_m) \quad (4)$$

where  $\vec{v}$  is the fluid velocity, and  $\vec{E}$  is the electric field related to the potential  $\Phi$  by  $\vec{E}(\vec{r}) = -\nabla\Phi(\vec{r})$ . Note that  $\vec{E}$  in equations (3) and (4) is in general the sum of any applied field  $\vec{E}_0$  and the self-field, or diffusion potential field, which exists if  $\bar{D}_+ \neq \bar{D}_-$ . The effect of convection on  $\vec{E}$  will be shown to be negligible for the case at hand. Finally,  $\vec{E}$  is related to the fixed and mobile charge species by Gauss' Law:

$$\nabla \cdot \epsilon \vec{E}(\vec{r}) = \rho_f \quad (5)$$

where  $\epsilon$  is the dielectric constant (assumed uniform) and  $\rho_f$  is related to the membrane volume fixed charge density  $\bar{\rho}_m$  and the mobile species concentrations by:

$$\rho_f(\vec{r}) = \bar{\rho}_m + F(\bar{c}_+(\vec{r}) - \bar{c}_-(\vec{r})) \quad (6)$$

Equations (1)–(6) constitute a complete description of the system if  $(\vec{v} - \vec{v}_m)$  is known. The problem of a rigid non-deformable membrane with  $\vec{v}_m = 0$  has been examined and numerical solutions exist for several special cases, e.g.  $\bar{D}_+ = \bar{D}_-$  with very high current densities only<sup>13</sup>, and<sup>7</sup>  $\vec{v} = 0$ . The effect of the change in intramembrane concentration on the

mechanical properties of the membrane was not of interest.

In the present context, it is illuminating to use a perturbation approach and examine a limiting case which yields a simple closed form solution. It is applicable for low and high current densities,  $\bar{D}_+ \neq \bar{D}_-$ , and  $(\vec{v} - \vec{v}_m) \neq 0$ . To assemble the system of interest, we consider a membrane whose fixed charge density is much greater than bulk solution concentrations which are initially equal,  $\bar{\rho}_m/F \gg c_0^1 = c_0^2$ . A Donnan equilibrium is assumed between membrane and bulk solutions, and for the case  $\bar{\rho}_m > 0$ ,  $\bar{\rho}_m$  is balanced by an equal amount of uniformly distributed mobile negative ions  $\bar{c}_{-0}$  in the membrane. If  $c_0^2$  were now increased slightly above  $c_0^1$  but remained  $\ll \bar{\rho}_m/F$ , and if  $\vec{E}_0$  were applied across the membrane, then additional mobile ions would enter or leave in perturbational amounts due to diffusion and migration, provided  $\vec{E}_0$  was much less than internal double layer fields which are<sup>14</sup>  $\sim 10^8$  V/cm. Defining the total intramembrane concentrations as the sum of equilibrium and perturbation concentrations  $\bar{c}_{\pm 0}$ ,  $\tilde{c}_{\pm}(x)$ , respectively:

$$\bar{c}_- = \bar{c}_{-0} + \tilde{c}_-(x) \quad (7)$$

$$\bar{c}_+ = \bar{c}_{+0} + \tilde{c}_+(x) \approx \tilde{c}_+(x) \quad (8)$$

$$\tilde{c}_-(x) \approx \tilde{c}_+(x) \ll \bar{c}_{-0} = \bar{\rho}_m/F \quad (9)$$

where  $\bar{c}_{+0} \approx 0$  in equation (8) can be interpreted in terms of Donnan exclusion of co-ions. The equalities in equation (9) represent the assumed quasi-neutrality condition, which more strictly is  $|\tilde{c}_+ - \tilde{c}_-|/\bar{c}_{-0} \ll 1$ . This condition is well justified if membrane thickness is much greater than a Debye length<sup>15</sup>  $1/\kappa$ ,

$$\delta \gg 1/\kappa = \left( \epsilon RT / \sum_i z_i^2 F^2 c_{i0} \right)^{1/2}$$

or equivalently, as long as the dielectric relaxation time in the membrane is much less than the diffusion time across the membrane. This is the case for all experiments to be presented here. The quasi-neutrality and perturbation inequality conditions in equation (9) together simplify the problem by decoupling Gauss' Law (5) from equations (1)–(4), recognizing that the electric field in the membrane is then approximately constant. The majority carriers ( $\bar{c}_{-0}$ ) effectively shield perturbation minority carriers so that no unbalanced space charge exists in the membrane which could give rise to  $\nabla \cdot \vec{E}$ . An applied field will not disturb electroneutrality as long as  $|\vec{E}_0|$  is much less than internal double layer field strengths. This approach is reminiscent of that taken in membrane electrodiffusion problems<sup>16,17</sup> and carrier flows in semiconductors<sup>18</sup>.

The problem is further simplified by focusing on the positive (minority) ions and recognizing that since  $\bar{c}_+ \ll \bar{c}_-$  and  $\bar{D}_+$  and  $\bar{D}_-$  are of the same order of magnitude, the positive ions are effectively shielded to the extent that the self-field migration term in equation (3) is negligible compared to the diffusion term; the self-field acts predominantly on the swamping amount of negative ions. However, as  $\vec{E}_0$  can be large, the applied field term cannot be neglected in equa-

tion (3). Since the radius of the collagen tube  $R \gg \delta$ , a one-dimensional model is well justified; combining equations (1), (3) and (8) with  $\nabla \rightarrow \partial/\partial x$ ,  $\vec{v} \rightarrow v_x$ ,  $\vec{E}_0 \rightarrow E_0$ , the  $x$ -directed field:

$$\frac{D\tilde{c}_+}{Dt} = \frac{\partial}{\partial x} \left( \bar{D}_+ \frac{\partial \tilde{c}_+}{\partial x} - [\bar{u}_+ E_0 + (v_x - v_m)] \tilde{c}_+ \right) \quad (10)$$

solution of which leads to the desired perturbation profile of mobile ions  $\tilde{c}_- \approx \tilde{c}_+$ . The boundary conditions on the perturbation concentrations at  $x = 0^+$  and  $x = \delta^-$ ,  $\tilde{c}_+(0^+)$  and  $\tilde{c}_+(\delta^-)$ , can be calculated from the rapidly established Donnan equilibrium<sup>17</sup>, where  $0^+$  and  $\delta^-$  are several Debye lengths from the edges of the membrane:

$$\tilde{c}_+(0^+) \approx (c_0^1)^2 / \bar{c}_{-0}; \quad \tilde{c}_+(\delta^-) \approx (c_0^2)^2 / \bar{c}_{-0} \quad (11)$$

where  $\bar{c}_{-0}$  is known from equation (9). The assumption in equation (11) that  $c_+(0^-) = c_0^1$  and  $c_+(\delta^+) = c_0^2$  requires an adequately stirred system.

At this point the relative importance of the convection and migration terms in equation (10) must be examined. An experimental and theoretical investigation<sup>11</sup> of electromechanical coupling with collagen membranes in the absence of a concentration gradient has led to relations between measured pressure and potential drops ( $\Delta P$ ,  $\Delta V$ ) across the membrane and measured total current and mass flow per unit area  $\vec{J}$  and  $(\vec{v} - \vec{v}_m)$  through the membrane which can be cast in the form:

$$\begin{bmatrix} \vec{n} \cdot (\vec{v} - \vec{v}_m) \\ \vec{n} \cdot \vec{J} \end{bmatrix} = \begin{bmatrix} L_{11} & L_{12} \\ L_{21} & L_{22} \end{bmatrix} \begin{bmatrix} \Delta P \\ \Delta V \end{bmatrix} \quad (12, 13)$$

where  $\vec{n}$ ,  $\vec{v}$  and  $\vec{J}$  are in the  $+x$  direction,  $\Delta V = V^2 - V^1$ ,  $L_{12} = L_{21} \approx 0$  for  $\bar{\rho}_m \approx 0$  and  $L_{22} < 0$ . The relations (12) and (13) are not significantly altered by the presence of the perturbation concentration gradient of interest. With  $\Delta P$  constrained to be zero (the experimental constraint imposed here), fluid flow can still occur via electromechanical coupling due to the imposed  $\vec{E}_0$ . Thus the convection term in equation (10) can be written in terms of  $\Delta V (= J/L_{22} = -E_0\delta)$  through equation (12). The ratio of the magnitudes of the convection and migration terms in equation (10) is then:

$$\frac{|L_{12}E_0\delta\tilde{c}_+|}{|\bar{u}_+E_0\tilde{c}_+|} = \frac{|L_{12}\delta|}{\bar{u}_+} \quad (14)$$

If the ratio in equation (14) is  $\ll 1$ , then the convection term can be neglected. A comparison of the remaining migration and diffusion terms in equation (10) shows that in the steady state, migration will totally dominate diffusion only if  $|E_0\delta| \gg RT/F$ . For the general case in which the convection term is included, equation (10) is easily solved in the steady state,  $D/Dt \rightarrow 0$ . For the cases  $E_0 = 0$  and  $E_0 \neq 0$  respectively, using equation (12) in equation (10) with  $\Delta P = 0$ :

$$\tilde{c}_+(x) = \tilde{c}_+(0^+) + [\tilde{c}_+(\delta^-) - \tilde{c}_+(0^+)]x/\delta \quad (15)$$

$$\tilde{c}_+(x) = \frac{[\tilde{c}_+(\delta^-) - \tilde{c}_+(0^+)] \exp [+E_0(1 - L_{12}\delta/\bar{u}_+)(x - \delta)/V_T] + \tilde{c}_+(0^+) - \tilde{c}_+(\delta^-) \exp [-E_0(1 - L_{12}\delta/\bar{u}_+)\delta/V_T]}{\{1 - \exp [-E_0\delta(1 - L_{12}\delta/\bar{u}_+)/V_T]\}} \quad (16)$$

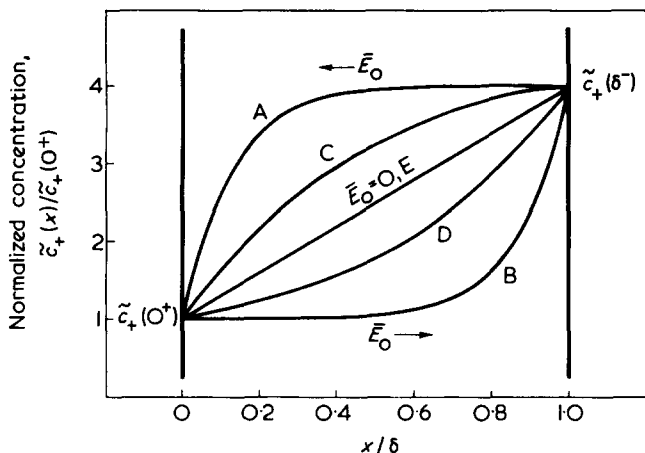


Figure 2 Normalized perturbation concentration  $\tilde{c}_+(x)/\tilde{c}_+(0^+)$  versus  $x/\delta$  inside a positively charged membrane of thickness  $\delta$ , calculated from equation (16) for the case  $\tilde{c}_+(\delta^-) = 4\tilde{c}_+(0^+)$ . A, B,  $|E_0\delta| = 8RT/F$ ; C, D,  $|E_0\delta| = 2RT/F$ ; E,  $E_0 = 0$ ; B, D,  $E_0 > 0$ ; A, C,  $E_0 < 0$

where  $V_T = RT/F$  is the equivalent thermal voltage  $\approx 25.7$  mV. Constraints other than  $\Delta P = 0$  can be handled easily using equations (12) and (13) together. Figure 2 shows the calculated, normalized concentration profile  $\tilde{c}_+(x)/\tilde{c}_+(0^+)$  corresponding to equations (15) and (16) for the case  $L_{12}\delta/\bar{u}_+ \ll 1$ , i.e. neglecting convection, which applies to the membrane used here (see Discussion). The plots are for  $E_0\delta = 0, \pm 2V_T, \pm 8V_T$ , with boundary concentrations  $\tilde{c}_+(\delta^-) = 4\tilde{c}_+(0^+)$ . We note that reversing the polarity of  $E_0$  in equation (16) has the effect of reversing the curvature of  $\tilde{c}_+(x)$ . When  $L_{12}\delta/\bar{u}_+ \gg 1$  the solution (16) is analogous to that plotted in Figure 2 but with the opposite sign of curvature. For the special case  $L_{12}\delta = \bar{u}_+$  the migration and convection effects cancel; the applied field therefore has no effect on the concentration profile and the profile (16) reduces to the linear profile (15) as if  $E_0 = 0$ . For a negatively charged membrane, the curvatures change sign for each of the respective cases above. Finally, given a model and prior experimental evidence for the way in which changes in intramembrane concentration lead to induced tensile forces in the fibril matrix<sup>5</sup>, the experimental results to be presented can be compared with the trends predicted by the theory outlined above (see Discussion).

## EXPERIMENTAL

Collagen tubing (dry radius 10.16 cm and wall thickness 0.0045 cm) was made from a dispersion of hide corium collagen as described by Lieberman<sup>20</sup> and kindly donated to us by Dr T. Tsuzuki, Devro Inc., Somerville, New Jersey. The tubing was extrusion cast and plasticized with a solution of glycerin and carboxymethyl cellulose; no cross-linking agent was added. Additional impurities (primarily natural fats) were present in an amount less than 0.5 wt %<sup>21</sup>. Examination of the fibrils prior to extrusion showed no loss of quaternary structure; after extrusion there was no detectable evidence of any fibril orientation in the extrusion direction<sup>21</sup> (the direction of the tube axis). All specimens were presoaked and rinsed several times with distilled water over a 24 h period to remove the plasticizing agent before use<sup>21</sup>. This tubing was among several samples previously used in our laboratory for studying electromechanical transduction properties of collagen<sup>11</sup>. Results of experiments with this tubing<sup>19</sup> will be compared to that obtained with an axially oriented extruded collagen fibre prepared from steer tendon<sup>22</sup>, as described in a previous paper<sup>5</sup>.

A length of tubing (15 cm) was clamped around two PMMA discs, one at each end, as sketched in Figure 1. The lower disc was fixed to the bottom of a 3 litre vessel and the top disc was connected to the load cell (Instron Engineering Corp., Canton, Mass.) whose output was displayed on an Instron chart recorder. The active cylindrical membrane area of  $\sim 121$  cm<sup>2</sup> separated inner and outer electrolyte baths at 23°C that were continuously pumped from large reservoirs at a rate fast enough to maintain independent, constant bulk concentrations in the face of ion migration and diffusion across the membrane, and to minimize the effects of boundary layers at the membrane edges. The volume of fluid inside the tube was  $\sim 120$  ml; inner and outer volumes were maintained constant for all experiments. The tube was initially stretched a small amount to obtain 100 g total baseline force, from which positive and negative force increments resulting from various stimuli could be measured.

In one series of experiments, the large reservoirs were disconnected and the outer and inner baths of 0.06 M NaCl were intermixed and continually recirculated from one to the other. Successive increments of 1.0 M HCl or NaOH were then added to the outer bath, each within less than 5 sec, in order to determine the force induced by changes in pH over a wide range. With recirculation the inner and outer baths attained equal pH approximately 0.5 min after each addition of reagent. In this and all other experiments, the pH was continuously monitored with a Radiometer digital pH meter PHM-63 which gave reproducible readings to  $\pm 0.01$  pH units. In another series with the same configuration, increments of 5 M NaCl were added to the bath which had an initial pH = 2.8 due to HCl, to determine the effect of neutral salt concentration on measured force. The initial ionic strength was due to HCl alone. Mixing time for the attainment of equal inner and outer NaCl concentration was again  $\sim 0.5$  min. All solutions were prepared from reagent grade chemicals. The force versus pH and neutral salt concentration experiments were performed as material characterizations to determine the maximum force that could be induced by electromechanochemical transduction for the given ultrastructure and orientation of the collagen specimen.

Steady electric fields were applied across the membrane via platinum electrodes as shown in Figure 1, to determine the effect on measured force. For the chosen configuration with tube radius much greater than membrane thickness  $R \gg \delta$ , the electric field inside the membrane was essentially uniform to a good approximation. Both the d.c. voltage applied to the electrodes and the current through the electrode-electrolyte-membrane circuit were measured. In all such experiments, the large reservoirs were used to isolate inner and outer baths so as to maintain specified NaCl concentration gradients across the membrane. The three gradients chosen were 0.002 M/0.012 M, 0.012 M/0.06 M, and 0.06 M/0.2 M, with initial pH  $\sim 2.8$  for both inner and outer baths. (The effect of  $E_0$  with gradients in pH was not studied.) As finite electrolysis rates could lead to changes in bath pH, fluid pumping rates were maintained fast enough so that the maximum such change that could occur in the vessel (i.e. for the maximum current density used in the experimental time period of interest) was less than 0.05 pH units away from the initial pH. Low current densities were used, the maximum being  $\sim 3$  mA/cm<sup>2</sup> in the membrane. Electrolysis caused negligible problems with the lowest of the three concentration combinations. However, with the highest combination, which yielded the highest

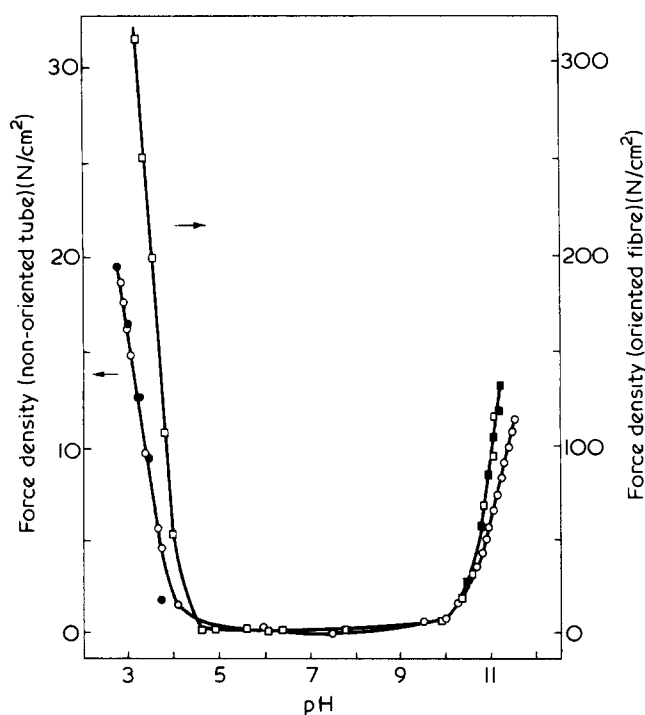


**Figure 3** Change in equilibrium isometric force density, referred to dry specimen cross-sectional area, about an initial stretching force over an extended pH range. ●, ○, Data for a single tube specimen with bath pH first decreased (●) and then increased (○); ■, □, data previously obtained<sup>5</sup> with an oriented collagen fibre shown for comparison; pH first increased, (■) then decreased (□). Ionic strength: 0.06 M (NaCl) at beginning of both experiments; less than 0.066 M at the end for each

current densities for a given electrode voltage, accumulation of gas limited the useful measurement time to  $\sim 5$  min for each application of a unit step in  $E_0 = J/(-L_{22})\delta = -\Delta V/\delta$ . As  $J$  rather than  $E_0$  or  $\Delta V$  was experimentally imposed, the data are plotted as a function of  $J$ .

## RESULTS

The results of the force *versus* pH and neutral salt concentration studies appear in *Figures 3* and *4*. The data of *Figure 3* represent the changes in force density induced by successive additions of acid or base, where force density is the measured force referred to the dry cross-sectional area of the specimen. The initial stretching force has been subtracted out in *Figure 3* and therefore the zero axis corresponds to the absence of a change in force density about the initial stretch. ○, ● Correspond to the collagen tube which has dry area =  $0.046 \text{ cm}^2$ . (For comparison, data are shown (□, ■) corresponding to previous measurements<sup>5</sup> performed in a like manner with an oriented collagen fibre having a dry cross-sectional area of  $8.32 \times 10^{-4} \text{ cm}^2$ .) With the tube immersed in a 0.06 M NaCl bath, the pH was initially lowered in steps to about 2.8 (●), then raised in steps to about 11.45 (○); total ionic strength increased by less than 10% over the entire course of the experiment which is thus considered as having been performed at approximately constant ionic strength. The change in force density *versus* time for all step changes in pH was monotonic. If we define a 'characteristic' time as that necessary for a force to reach some reference percentage, say  $1 - 1/e$  or 63% of the asymptotic force level, we observe the following: the characteristic times were longest ( $\sim 11$  min) at pH values

$\sim 4$  and 10.5, and gradually became shorter as the pH was decreased below 4 and increased above 10.5 (as short as 2–3 min). They were shortest and sometimes barely detectable in the neutral pH range. This general behaviour is similar to that previously found with collagen fibres<sup>5</sup>. It was found that the equivalent force densities available with an oriented fibre were more than an order of magnitude larger than that with the randomly oriented tube.

The effect of neutral salt concentration at constant acidic pH is summarized in *Figure 4*, corresponding to experiments with the same specimens as those of *Figure 3*. These data show the change in force density after successive additions of NaCl, once again with the initial stretching force subtracted. In each experiment the initial step was the adjustment of the acidic pH using HCl and the attainment of the corresponding equilibrium force. The first data point in each curve refers to this force and the anion ( $\text{Cl}^-$ ) concentration due to HCl alone. Subsequent addition of NaCl with both specimens led to changes in force that were not monotonic in time; rather there ensued an initial decrease followed by a slower increase whose asymptotic value was larger than the previous equilibrium state. This is clearly seen in *Figure 5a*, which corresponds to the transition between the first and second fibre data points of *Figure 4*. Similar behaviour was observed with the tube specimen for points up to  $\sim 0.025$  M; the characteristic time for the secondary increase in force was  $\sim 2.5$ –4 min. After a certain anion concentration was reached (typically that of the maxima in the curves of *Figure 4*,  $\sim 0.025$  M for the tube and  $\sim 0.002$  M for the fibre specimens), further additions of NaCl were accompanied by only the initial, relatively fast decrease in force with no subsequent slow increase as before. The force was found to decrease continuously with increasing anion concentration after this point (see *Figure 4*). In this latter region of the curve, the characteristic time for each decrease in force was typically 50 sec or less for the case of the collagen tube. Approximately 30 sec of this time was attributable to bath mixing

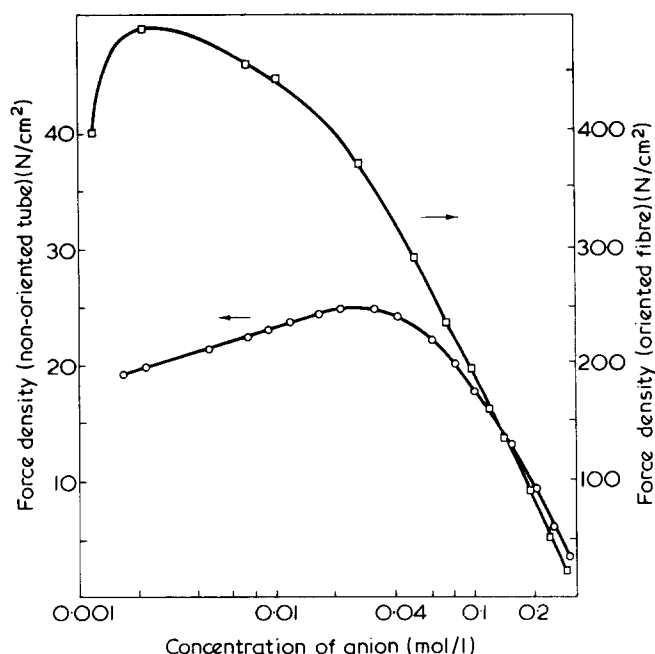


**Figure 4** Change in isometric force density due to successive increments in NaCl at constant pH: ○, tube pH = 2.8; □, fibre<sup>5</sup>, pH = 2.93

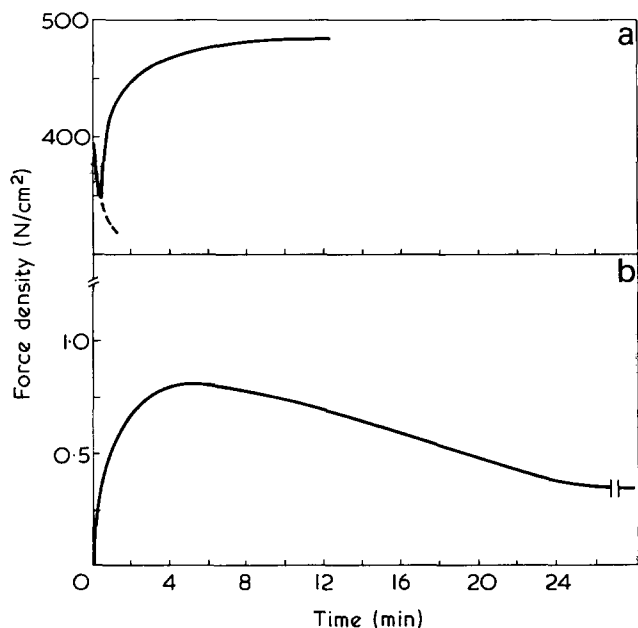


Figure 5 (a) Change in force density after a single step increase in NaCl concentration for an oriented fibre initially in a bath at pH 2.93 with no neutral salt. Final chloride ion concentration = 0.002 M. (b) Electromechanochemically induced change in force density in response to a single step jump in  $J$  for a low applied  $J = 0.12 \text{ mA/cm}^2$ ;  $c_0^1 = 0.002 \text{ M}/c_0^2 = 0.012 \text{ M NaCl}$ ; pH = 2.8

after pipetting of reagent. (The equivalent time for the fibre was 12 sec including a  $\sim 5$  sec mixing time.)

The quantitative response of the collagen tube to an electric field (imposed  $J$ ) is summarized in Figure 6. Representative data are shown corresponding to five experiments with the same specimen using positive and negative  $J$  with the three concentration gradients chosen. In each experiment, the initial step was the establishment of the concentration gradient with both inner and outer baths at the same pH = 2.8. This resulted in a corresponding equilibrium force density. A step jump in  $J$  was then applied and turned off after 5 min. This was followed by another turn-on, turn-off cycle. The data of Figure 6 are the changes in force density attained after  $J$  had been on for 5 min and a new steady state force had been reached; the initial equilibrium force density has once again been subtracted. It is important to note that a positive force density was induced in all cases when  $c_0^2 > c_0^1$  and  $J$  (or  $E_0$ ) was positive,  $E_0 > 0$  defined as pointing from outside to inside across the membrane. Reversing the polarity of  $E_0$  with  $c_0^2 > c_0^1$  reversed the polarity of the induced force density. For all cases in which  $c_0^2 < c_0^1$ ,  $E_0 > 0$  induced negative forces and conversely. The characteristic times for the turn-on transients, that is, the transient change in force after  $J$  was turned on, were in the range of 36–80 sec. With all three concentration gradients, the turn-on time constant was found to decrease as the value of the applied  $J$  was increased, in some experiments by as much as 50% for the range of  $J$  used. For each turn-on, turn-off cycle, the turn-off time constant was invariably longer than the turn-on time constant, in some cases by a factor of 2 or 3. From a comparison of such time constants it has been estimated (see Discussion) that the values of applied  $|\Delta V| = |E_0 \delta|$  used in these experiments, corresponding to the current densities used, are in the range 0 to  $\sim 10RT/F \approx 250 \text{ mV}$ .

Finally in another series of experiments with  $c_0^1 = 0.012 \text{ M}$  and  $c_0^2 = 0.002 \text{ M NaCl}$  at pH = 2.8 (i.e. the lowest concen-

tration combination of the three), the applied current was left on for 30 min for several different values of  $J$ . It was found that typically 6–8 min after turn-on, a slow drift in force occurred which lowered the force below the level corresponding to the 5 min 'asymptotic' value, as shown in Figure 5b. As previously mentioned, problems due to electrolysis prevented equivalent long term measurements with the higher concentration combinations.

## DISCUSSION

A model which would adequately explain the observed effect of an electric field on tensile forces in collagen can be constructed on the known internal electrostatic interactions inherent to collagen in aqueous media with no applied field<sup>4,5,29</sup> the trends predicted by the theoretical treatment above, and the ultrastructural features<sup>23,24</sup> of the collagen specimens. The tubing films used in the present electromechanical studies have fibril orientation which is random in the plane of the film, while the fibres can be considered as having a network of fibrils which are highly oriented in the direction of fibre axis. In addition, previous experiments<sup>11</sup> have shown that the film acts as a permeable membrane through which water and small ions can be transported. In the range of pH and ionic strength studied, the tertiary structure of the fibres and films is predominantly unaltered at 23°C<sup>24,5</sup>. When bath pH is shifted away from the isoelectric point, both specimens attain a net primary or 'fixed' charge according to well accepted notions<sup>25,26</sup>. The exact spatial distribution of mobile counter ions, i.e. the electrical double layer, depends on the spatial geometry of the primary charge. With charged fibres in the absence of an applied electric field, interaction between double layers has

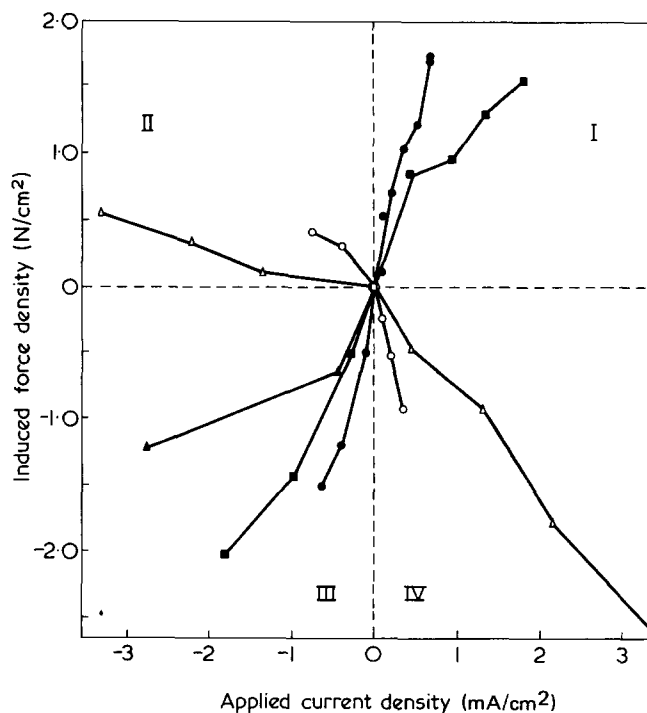


Figure 6 Representative electromechanochemical coupling data obtained with a collagen tube in the acidic region supporting gradients in NaCl concentration having the values: ●,  $c_0^1 = 0.002 \text{ M}/c_0^2 = 0.012 \text{ M}$ ; ○,  $c_0^1 = 0.012 \text{ M}/c_0^2 = 0.002 \text{ M}$ ; ■,  $c_0^1 = 0.012 \text{ M}/c_0^2 = 0.06 \text{ M}$ ; ▲,  $c_0^1 = 0.06 \text{ M}/c_0^2 = 0.2 \text{ M}$ ; △,  $c_0^1 = 0.2 \text{ M}/c_0^2 = 0.06 \text{ M}$ ; applied current density  $J$  is related to  $E_0$  by equation (13) of text. Force density is referred to membrane cross-sectional area and current density to cylindrical surface area.

been found to produce repulsive forces which are strongest, because of the predominantly axial orientation, in the direction normal to the fibre axis<sup>5</sup>. These lateral repulsive forces are converted by the fibril matrix to macroscopic axial forces. The same repulsive forces exist in the charged collagen tube, as is evidenced by visible swelling in the lateral direction when the pH is shifted away from the IEP. However, because of the one fewer degree of orientation, one would expect in general that the summed effect of such repulsive forces would lead to axial macroscopic force densities smaller than that of a comparable cross-sectional area of oriented fibres.

That these lateral repulsive forces can give rise to isometric axial forces in the collagen tubing is seen in the data of Figures 3 and 4; the trends of these data are very similar to those of the collagen fibres. Thus in Figure 3 an increase in net positive or negative charge at low or high pH respectively and at constant ionic strength (constant Debye length) gives rise to an increase in force density independent of the sign of the charges. The force density induced in the tube is typically about 25 times less than that of the fibre at a given pH; the pH of zero induced force density can be considered a measurement of the IEP for those insoluble collagen specimens<sup>5</sup>. Finally, the long characteristic times associated with changes in tube force density due to step changes in pH (2–11 min; see Results) can be understood in terms of the diffusion limited chemical reaction<sup>27,28</sup> that takes place upon addition of HCl or NaOH to the bath. These experimental times will henceforth be referred to as  $\tau_{H^+}$ .

The force density versus anion concentration data show that two electrostatically mediated events, whose effects are to produce forces of opposite polarity (direction), can occur simultaneously. An increase in concentration of a relatively non-binding or non-reacting salt (e.g. NaCl<sup>29</sup>) at constant pH leads to a decrease in internal Debye lengths at a rate governed by ionic diffusion into the matrix, as represented by the characteristic diffusion time  $\tau_{diff} \sim \delta^2/2D$ . (The dielectric relaxation time  $\tau_e = \epsilon/\sigma$  for reordering of the ionic atmospheres once diffusion has occurred is  $\sim 10^{-7}$ – $10^{-9}$  sec which is  $\ll \tau_{diff}$ , where  $\sigma$  is conductivity.)  $\tau_{diff}$  should theoretically be less than  $\tau_{H^+}$ ; for the tubing,  $\tau_{diff}$  is calculated to be  $\sim 15$ – $20$  sec. The diffusion limited decrease in  $1/\kappa$  leads at first to a concomitantly fast decrease in force (e.g. Figure 5a). It is well known from titration studies, however, that such a manifestation of electrostatic interaction between protein side groups can lead to a change in dissociation equilibrium for collagen<sup>25,26,30</sup> and other polyelectrolytes<sup>31</sup>; in this case the increase in bath concentration could lead to an increase in the fraction of groups dissociated<sup>25,30</sup>. Such an increase in net charge would in fact lead to the secondary rise in force seen in Figure 5a and also found with the tube. The fact that the initial decrease in force is found to occur in a time  $\sim \tau_{diff}$  and that the secondary increase occurs in a time  $\sim \tau_{H^+}$  (see Results) both for the tube and the fibre supports this view. Therefore, the initial quick decrease in double layer repulsion can be considered the result of a decrease in  $1/\kappa$  at approximately constant collagen charge, which is followed by a slow increase in charge at the new, constant  $1/\kappa$ . This force vs. time dependence is seen for the tube up to  $\sim 0.025$  M. Above this concentration, the absence of any slow secondary change in force suggests that collagen charge has remained constant even with further addition of salt at the given bath pH<sup>30</sup>. The continued occurrence of the

initial decrease in force as additional salt is added shows, however, that the first electrostatic effect is still present; this is again supported by the experimental time constants which are  $\sim \tau_{diff}$ . The importance of the various time constants characterizing the physical processes found in the 'baseline experiments' of Figures 3–5a is stressed in order to establish one context in which to examine the electric field-induced forces. Parenthetically, it appears that such macroscopic measurements provide significant insight into the study of certain electrically mediated rate processes affecting collagen at the ultrastructural level.

In order to interpret the trends of the electromechanochemical transduction data of Figure 6, we focus on the polarity of the induced force as a function of the polarity of  $E_0$  given the relative magnitudes of  $c_0^1$  and  $c_0^2$ , the magnitude of the induced force compared to previously found electrokinetically induced forces<sup>5,11</sup>, the time constants associated with the present  $E_0$ -induced forces, the three ranges of concentration gradient used, and the force data of Figures 4 and 5. These trends are compared with those predicted by the theoretical model presented above. With respect to the latter, we recall that equation (16) and Figure 2 have been derived for the case  $\bar{\rho}_m/F \gg c_0^1, c_0^2$ . Schlogl<sup>13</sup> has given numerical calculations for the case  $\bar{\rho}_m/F$  slightly less than bulk concentrations, with  $v_m = 0, D_+ = D_-$  ( $\vec{E}_{self} \equiv 0$ ), and large  $J$  (or  $E_0$ ). The trends of the latter solution are identical with those predicted by equation (16) in the frame of the membrane, concerning the way in which intramembrane concentration can be increased or decreased by  $E_0$ , with or without significant convection. The actual experiments (Figure 6) fall roughly between these two limits as  $\rho_m/F \lesssim 0.1$  M for the electrolyte conditions used<sup>28</sup>. In addition, measurements<sup>11</sup> on the collagen tube used here have shown that the ratio in equation (14) is less than  $10^{-2}$  (with the assumption that co-ion mobility is not significantly different from that in bulk solution<sup>8</sup>); therefore convection in equation (16) can be neglected and we will use equation (16) and Figure 2 for ease of comparison with our experimental data.

All the experiments in Figure 6 show induced force density polarities which can be interpreted in terms of the hypothesis that a change in mean intramembrane salt content leads to a concomitant change in  $1/\kappa$  and hence a change in lateral repulsion forces and total force density. In quadrant I of Figure 6, for example, a positive  $J$  induces positive force; the larger the  $J$ , the larger the force. Equation (16) and Figure 2 predict that a positive  $E_0$  with  $c_0^2 > c_0^1$  causes a decrease in mean intramembrane salt content (and therefore an increase in  $1/\kappa$ ); the larger the  $E_0$  the less the mean salt content. Reversing the polarity of  $E_0$  conversely leads to an increase in salt concentration. Such a prediction is in accordance with the observation of a negative induced force as seen in all the data in quadrant III of Figure 6. When  $c_0^1 > c_0^2$  (quadrants II and IV) the polarity of the induced force versus  $E_0$  was found to be opposite that of the previous cases (quadrants I and III). These observations can also be interpreted in an identical fashion with respect to Figure 2. This reversal appears to cancel, by itself, the possibility that the observed forces might be caused primarily by a simple electrokinetic (e.g. electrophoretic) 'push' on the membrane, an effect which has been observed in the past in homogeneous electrolyte baths<sup>5,11</sup>. Simply switching the inner and outer baths (i.e. reversing the concentration gradient) without changing the sign of  $\bar{\rho}_m$  would not lead to a reversal in force polarity for the same  $E_0$  based

on an electrokinetic interpretation. Further, the magnitude of electrokinetically induced force densities has been found to be less by almost an order of magnitude<sup>5</sup> than those of *Figure 6*, for an equivalent  $E_0$ .

The proposed hypothesis is entirely unambiguous in the case of the 0.06 M/0.2 M data ( $\Delta$ ,  $\blacktriangle$ ) of *Figure 6*, since the equilibrium force density of curve of *Figure 4* (for the collagen tube) shows an inverse relationship with concentration in this range. Qualitatively,  $E_0$  might be construed as a means of constraining the total force density to follow a path defined by this part of the curve. However, such an argument would not coincide with the observed proportionality of the equilibrium force (cf. *Figure 4*) in the range 0.002–0.025 M. To reconcile these observations, the detailed time response of the  $E_0$ -induced force in this low concentration range must be examined (see *Figure 5b*). We first note that the initial changes in  $E_0$ -induced force for all the experiments of *Figure 6*, including the low concentration ranges, were characterized by time constants  $\tau_{E_0} \sim 36$ –80 sec (see Results), which are roughly on the order of calculated  $\tau_{\text{diff}}$ . This in itself is further evidence that induced changes in intramembrane concentration are initially at work, as opposed to (for example) diffusion limited reaction processes which would accompany an  $E_0$ -induced change in pH. The slow reversal in force (with a time in the range  $\sim\tau_{H^+}$ ) seen in *Figure 5b* can be interpreted once again as a change in dissociation and hence a slow charging process, in this instance due to the  $E_0$ -induced change in neutral salt concentration. Such a reversal is in accordance with the interpretation of *Figure 5a*, the low concentration data of *Figure 4*, and the known charging properties of collagen<sup>30</sup>. However, the data of *Figure 6* correspond to the 5 min 'steady state' force densities attained before such secondary force reversals are seen to occur. We conclude that since  $\tau_{E_0} \sim \tau_{\text{diff}} \ll \tau_{H^+}$ , the data of *Figure 6* with the low ionic strength combinations should not be interpreted via the long time equilibrium curve of *Figure 4* in the equivalent concentration range, but rather are consistent with the proposed hypothesis.

The relationship between  $\tau_{E_0}$  and  $\tau_{\text{diff}}$  can be examined further in the context of the limiting model for electromechanochemical transduction embodied in equation (10). The full transient solution of equation (10) in the case of negligible convection ( $\partial/\partial t \neq 0$ ,  $\vec{v} = \vec{v}_m = 0$ ) has been given with respect to squid axon electrodiffusion problems<sup>16</sup> in terms of a Fourier superposition with a governing time constant for the establishment of the steady state concentration profile; the latter can be cast in the form<sup>16</sup>:

$$\tau = \tau_{\text{diff}} \left[ \frac{1}{1 + \left( \frac{|E_0 \delta|}{\pi V_T} \right)^2} \right] \quad (17)$$

The characteristic times for  $E_0$ -induced forces  $\tau_{E_0}$  should thus be directly related to the  $\tau$  of equation (17) according to the present hypothesis. Equation (17) thus suggests that the turn-on time  $\tau_{E_0} \propto \tau$  ( $E_0 \neq 0$ ) for force transients should be less than the turn-off time  $\propto \tau$  ( $E_0 = 0$ ) =  $\tau_{\text{diff}}$ . This has in fact been observed (see Results). In addition, equation (17) predicts that  $\tau_{E_0}$  should decrease with increasing  $E_0$ , which has also been observed. (Measurements of  $L_{22}$  are currently in progress to compare the  $\Delta V$  predicted by equation (17) with that calculated from  $\Delta V = J/L_{22}$ .) Therefore, diffusion is not rate limiting for  $E_0 \neq 0$ .

Several additional comments are in order concerning the data of *Figure 6*. If a highly oriented tube were used in the present configuration, then force densities  $\sim 25$  times larger could be obtained; thus a 4 N/cm<sup>2</sup> excursion obtained by switching from  $+E_0$  to  $-E_0$ , say, on the curves of *Figure 6* would translate to  $\sim 100$  N/cm<sup>2</sup>. Second, a curve of force density versus  $|E_0|$  should in general be non-linear and should saturate for high enough  $E_0$ , given the known upper and lower intramembrane concentration limits defined by  $c_0^1$  and  $c_0^2$ . This can be seen in the trends of the theoretical curves of *Figure 2*. Finally, although the curves of *Figure 2* predict antisymmetric concentration profiles for  $+E_0$  and  $-E_0$  about the profile for  $E_0 = 0$ , the profiles and therefore forces are in general not symmetric when the conditions  $\bar{\rho}_m/F \gg c_0^1, c_0^2$  are not satisfied<sup>13</sup>.

In conclusion, examination of the trends of electromechanochemical transduction experiments viewed in the context of a theoretical model appear to confirm the feasibility of such a transduction process, in which an applied  $E_0$  is used to control intramembrane concentration profiles thereby inducing tensile forces. The isometric force densities involved are not insignificant by analogy to those of striated muscle. Characteristic times for the transduction process can be made much smaller than that observed here by proper material design, e.g. by using much thinner membranes which could be overlapped so as to maintain sufficient cross-section and therefore significant total forces. The use of multivalent ions might allow the use of much smaller concentration gradients as very small amounts can lead to large changes in force<sup>5</sup>. The collagen can be chemically modified, or collagen/glycosaminoglycan composites or other polyelectrolytes can be used for the purpose of having a material which is charged at physiological pH<sup>28</sup>. Such a transduction process can also be used to make possible electric field-control of internal concentrations of salts which have specific effects on the material, e.g. salts involved in partly reversible denaturation<sup>1–3</sup>.

The experiments presented in this paper show that electric field-induced changes in the microscopic structure of a polyelectrolyte such as collagen can be harnessed to yield, on the one hand, a macroscopic force and the concomitant performance of mechanical work. On the other hand, such changes in membrane architecture at the ultrastructural level should also manifest themselves in altered hydrodynamic and ionic permeabilities. Thus the transduction mechanisms of interest here may also have important implications concerning the possibility of altering transport across polyelectrolyte membranes by, for example, electrically induced changes in equivalent pore size. An investigation of such effects is now in progress.

#### ACKNOWLEDGEMENTS

The authors are grateful to Professors I. V. Yannas, J. R. Melcher and Dr M. J. Glimcher for helpful discussions, and to Professor Yannas for the use of his laboratory facilities. The work has been supported in part by NSF Grant ENG74-09744 and Health Sciences Fund Grant 77-02.

#### REFERENCES

- 1 Steinberg, I. Z., Oplatka, A. and Katchalsky, A. *Nature* 1966, 210, 568
- 2 Rubin, M., Piez, K. A. and Katchalsky, A. *Biochemistry* 1969, 8, 3628
- 3 Yonath, J. and Oplatka, A. *Biopolymers* 1968, 6, 1129



*Tensile forces in collagen: electromechanochemistry: A. J. Grodzinsky and N. A. Shoenfeld*

- 4 Katchalsky, A., Lifson, S., Michaeli, I. and Zwick, M. in 'Size and Shape of Contractile Polymers,' (Ed. A. Wasserman), Pergamon, London, 1960
- 5 Yannas, I. V. and Grodzinsky, A. J. *J. Mechanochem. Cell Motility* 1973, 2, 113
- 6 Vander, A. J., Sherman, J. H. and Luciano, D. S. 'Human Physiology – The Mechanisms of Body Function', McGraw Hill, New York, 1970, p 229
- 7 Teorell, T. *Prog. Biophys. Biophys. Chem.* 1953, 3, ch 9
- 8 Kobatake, Y. and Kamo, N. *Prog. Polym. Sci. Japan* 1973, 257
- 9 Hills, G. J., Jacobs, P. W. M. and Lakshminarayanaiah, *Proc. Roy. Soc. (A)* 1961, 262, 246
- 10 Sollner, K. J. *Macromol. Sci. (A)* 1969, 3, 1
- 11 Grodzinsky, A. J. and Melcher, J. R. *IEEE Trans. Biomed. Eng.*, 1976, BME-23, 421
- 12 Teorell, T. *J. Gen. Physiol.* 1959, 42, 847
- 13 Schlögl, R. and Schödel, U. *Z. Physik. Chem. (Frankfurt)* 1955, 5, 372
- 14 Alexandrowicz, A. and Katchalsky, A. *J. Polym. Sci. (A)* 1963, 1, 2093
- 15 Agin, D. *Proc. Nat. Acad. Sci.* 1967, 57, 1232
- 16 Cole, K. S. *Physiol. Rev.* 1965, 45, 340
- 17 Helfferich, F. 'Ion Exchange,' McGraw-Hill, New York, 1962, Ch.8
- 18 Adler, R. B., Smith, A. C. and Longini, R. L. 'Introduction to Semiconductor Physics', Wiley, New York, 1964, Ch.4
- 19 Shoenfeld, N. A. and Grodzinsky, A. J. *Proc. First Cleveland Symposium on Macromolecules October 1976* in press; Shoenfeld, N. A. *S.B. Thesis MIT* (1976)
- 20 Lieberman, E. R. US Pat. 3 123 482 (1964)
- 21 Tsuzuki, T. Personal communication
- 22 Oneson, I., Fletcher, D., Olivo, J., Nichols, J. and Kronenthal, R. K. *J. Am. Leather Chem. Assoc.* 1970, 65, 440
- 23 Yannas, I. V. *Rev. Macromol. Chem. (C)* 1972, 7, 49
- 24 Traub, W. and Piez, K. A. *Adv. Protein Chem.* 1971, 26, 243
- 25 Bowes, J. H. and Kenten, *Biochem. J.* 1948, 43, 358
- 26 Veis, A. in 'Treatise on Collagen', Academic Press, London, 1967, Vol.1, Ch.8
- 27 Overbeek, J. Th. G. Personal communication
- 28 Picheny, M. A. and Grodzinsky, A. J. *Biopolymers* 1976, 15, 1845
- 29 Li, S. T. and Katz, E. P. *Biopolymers* 1976, 15, 1439
- 30 Gustavson, K. H. 'The Chemistry and Reactivity of Collagen,' Academic Press, New York, 1956, p 87
- 31 Timasheff, S. N. *Biol. Macromol.* 1970, Series 3, 1